Volume 31 Number 14 15 September 2011 ISSN 0278-4343

ELSEVIER

CONTINENTAL SHELF RESEARCH

Continued on outside back cover

www.elsevier.com/locate/csr

Continental Shelf Research 31 (2011) 1527–1540

Contents lists available at ScienceDirect

Continental Shelf Research

journal homepage: www.elsevier.com/locate/csr

Research papers

Comparisons of picophytoplankton abundance, size, and fluorescence between summer and winter in northern South China Sea

Bingzhang Chen [a,b], Lei Wang [b], Shuqun Song [a,c], Bangqin Huang [b], Jun Sun [d], Hongbin Liu [a,*]

[a] Division of Life Science, Hong Kong University of Science and Technology, Clear Water Bay, Kowloon, Hong Kong
[b] State Key Laboratory of Marine Environmental Science, Environmental Science Research Center, Xiamen, PR China
[c] Key Laboratory of Marine Ecology and Environmental Science, Institute of Oceanology, Chinese Academy of Sciences, Qingdao, PR China
[d] College of Marine Science and Engineering, Tianjin University of Science and Technology, Tianjin, PR China

ARTICLE INFO

Article history:
Received 29 December 2010
Received in revised form
26 June 2011
Accepted 30 June 2011
Available online 12 July 2011

Keywords:
Picophytoplankton
Abundance
Size
Fluorescence
South China Sea
Seasonal comparison

ABSTRACT

The abundance, size, and fluorescence of picophytoplankton cells were investigated during the summer (July–August of 2009) and winter (January of 2010) extending from near-shore coastal waters to oligotrophic open waters in northern South China Sea, under the influence of contrasting seasonal monsoons. We found that the median abundance of *Prochlorococcus* averaged over top 150 m decreased nearly 10 times in the winter compared to the summer in the whole survey area, while median abundance of *Synechococcus* and picoeukaryotes increased 2.6 and 2.4 folds, respectively. Vertical abundance profiles of picoeukaryotes usually formed a subsurface maximum during the summer with the depth of maximal abundances tracking the depth of nutricline, whereas their vertical distributions were more uniform during the winter. Size and cellular fluorescence of *Prochlorococcus* and *Synechococcus* usually increased with depth in the summer, while the size of picoeukaryotes was smallest at the depth of maximal abundances. Size, cellular fluorescence, and chlorophyll-to-carbon ratio of *Prochlorococcus* and *Synechococcus* in surface waters were generally higher in the winter than in the summer and onshore than offshore, probably resulting from different temperature, nutrient, and light environments as well as different ecotype compositions. *Prochlorococcus* cells were most abundant in warm and oligotrophic environments, while the abundance of *Synechococcus* and picoeukaryotes was the highest in waters with intermediate chlorophyll and nutrient concentrations. The distributional patterns of picophytoplankton groups are consistent with their specific physiology documented in previous studies and can be possibly predicted by environmental physical and chemical variables.

1. Introduction

South China Sea (SCS) is the largest marginal sea in southeastern Asia and plays important roles in regulating regional climate and carbon budget owing to its vast area and volume. Although the near-shore waters on the shallow shelf can be affected by riverine discharge and coastal upwelling, the central part of SCS is usually oligotrophic, with macronutrient concentrations below the detection limit and possibly iron limitation (Wu et al., 2003; Wong et al., 2007). Compared with oligotrophic gyres in North Pacific and North Atlantic at similar latitudes, SCS is characterized by smaller size and shallower depths of nutricline, mixed layer, and chlorophyll maximum (Liu et al., 2002b; Wong et al., 2007). As such, picophytoplankton (<3 μm), namely *Prochlorococcus* (Pro), *Synechococcus* (Syn), and picoeukaryotes (Peuk), constitutes an essential component of phytoplankton in SCS (Ning et al., 2005; Liu et al., 2007).

The physical and chemical environments in the upper ocean layer of SCS are primarily affected by Eastern Asian monsoons (Wang et al., 1999). During the winter, the northeast monsoon brings cold air from the continent, cools down the sea surface temperature (SST), deepens the surface mixed layer, and entrains nutrients into the surface ocean layer, stimulating biological production (Chen and Chen, 2006). The upper ocean layer in northern SCS forms a large-scale cyclonic eddy under the influence of the northeast monsoon and the nutrient-rich East China Sea coastal water can flow into northern SCS via the Taiwan Strait, while during the summer, the southwest monsoon prevails and the water circulation in the upper ocean layer forms an anticyclonic eddy with some SCS water entering the East China Sea via the Taiwan Strait (Fang et al., 1998; Hu et al., 2000). The southwest winds also induce offshore Ekman transport and coastal upwelling along the South China coast (Gan et al., 2010). With higher discharge in the summer than in the winter, Pearl

* Corresponding author. Tel.: +852 2358 7341; fax: +852 2335 9317.
E-mail address: liuhb@ust.hk (H. Liu).

0278-4343/$ - see front matter © 2011 Elsevier Ltd. All rights reserved.
doi:10.1016/j.csr.2011.06.018

River brings large amounts of inorganic nutrients as well as terrestrial organic matters into the northern SCS. The SCS is also subject to the influence of frequent passage of typhoons and internal waves (Liu et al., 1998). The seasonality of nutrients, Chl *a* concentration, and primary production in SCS induced by changes in physical forces has been investigated by a number of studies (Liu et al., 2002b; Ning et al., 2004; Chen and Chen, 2006), which usually show that phytoplankton standing stocks, primary production, and new production peak during the wintertime when surface mixed layer deepens and nutrients are entrained into the euphotic zone. Previous studies on picophytoplankton biomass in SCS are often limited in spatial and temporal coverage. For example, Liu et al. (2007) investigated two annual cycles of picophytoplankton dynamics at a basin station (SEATS), showing that *Synechococcus* cells usually bloom during the winter. Ning et al. (2005) provided a synoptic picture of picophytoplankton community structure at some coastal and oceanic stations over the western part of northern SCS during the summer of 2005. Pan et al. (2006) investigated the changes in picophytoplankton community along one transect (the same as Transect A in this study) during the winter of 2004.

Our objective in this study is to see whether and how the contrasting physical and chemical environments between summer and winter affect the abundance, single-cell properties such as size and cellular fluorescence of the three picophytoplankton groups with an unprecedented spatial coverage in northern South China Sea. More specifically, will the expected nutrient enrichments induced by greater mixing in the winter increase the abundance, size, and cellular fluorescence of picophytoplankton cells as for total chlorophyll concentration? The data provided in this study can also facilitate further work aiming to estimate phytoplankton biomass using mechanistic models coupled with physical dynamics (Gan et al., 2010) or remote-sensing techniques.

2. Methods

Two milliliter seawater samples were collected at 3–12 depths from the upper 150 m using Niskin bottles attached to a CTD rosette system during the summer (July 18–August 16, 2009; 79 stations) and winter (January 6–30, 2010; 63 stations) in SCS. The samples were fixed with seawater buffered paraformaldehyde (0.5% final concentration) and stored at −80 °C until analysis. Upon return to the lab, cell abundances of picophytoplankton were enumerated using a Becton-Dickson FACSCalibur cytometer, with different populations distinguished based on side-scattering, orange and red fluorescence using WinMDI 2.9 developed by Joseph Trotter (Olson et al., 1993). As a total volume of only 150 μl was analyzed, the upper size limit for picoeukaryotes was usually 3 μm, above which the cells were very rare and could not be accurately quantified. Yellow-green fluorescent beads (1 μm, Polysciences) were added to each sample as an internal standard. The exact flow rate was calibrated by weighing a tube filled with distilled water before and after running for certain time intervals and the flow rate was estimated as the slope of a linear regression curve between elapsed time and weight differences (Li and Dickie, 2001).

Cellular biovolumes and equivalent spherical diameters (ESD) of plankton were roughly estimated from side-scattering (SS) normalized to 1 μm beads using an empirically determined power-law equation following Durand et al. (2001), Worden et al. (2004), and Bec et al. (2008) (Fig. 1A). According to the Mie theory, the volume of small particles can be described as a power-law function of light scattering (Morel, 1991). Cellular biovolumes of nine species in exponential growth phase (*Synechococcus* WH7803, *Synechococcus bacillaris* CCMP1333,

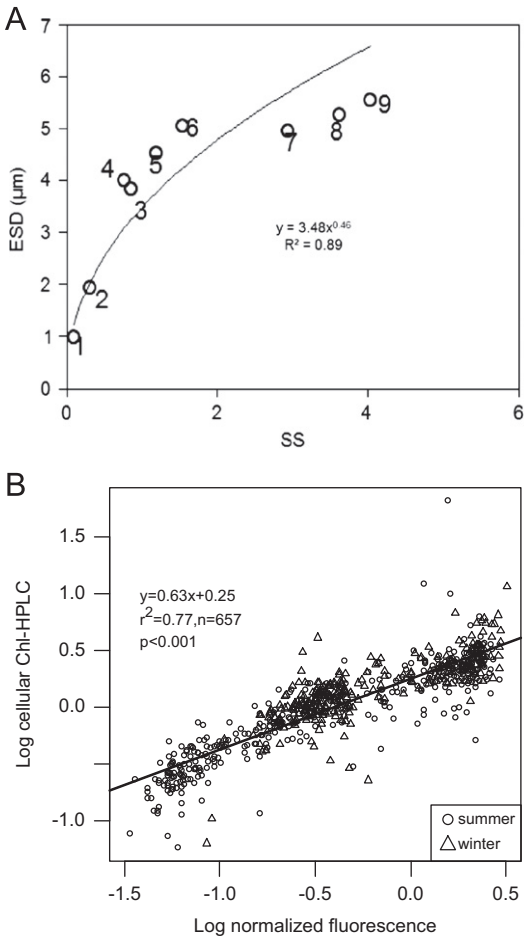

Fig. 1. Empirical equations converting (A) normalized side scattering to equivalent spherical diameters (ESD) for nine phytoplankton cultures and (B) normalized red fluorescence of *Prochlorococcus* to cellular divinyl Chl *a* content measured by HPLC. The numbers labeling data points in (A) represent each specific alga strain used: 1: *Synechococcus* WH7803; 2: *Synechococcus bacillaris* CCMP1333; 3: *Chlorella autotrophica* CCMP243; 4: *Chlorella* sp.; 5: *Aureoumbra lagunensis* CCMP1508; 6: *Isochrysis galbana*; 7: *Aureoumbra lagunensis* (TBA2); 8: *Nannochloropsis* sp.; and 9: *Pavlova lutheri.*

Chlorella sp., *Pavlova lutheri*, *Isochrysis galbana*, *Chlorella autotrophica* CCMP243, *Nannochloropsis* sp., *Aureoumbra lagunensis* CCMP1508, and another strain of *Aureoumbra lagunensis* (TBA2, provided by Hudson R. DeYoe, University of Texas—Pan American)) were determined using a Z2 particle counter (Beckman Coulter) and their SS after the same fixation procedure as for field samples were determined on the same cytometer. Cellular carbon content of picophytoplankton cells was estimated from cellular biovolume by assuming conversion factors of 0.28 pg C μm^{-3} for Pro and Syn and 0.22 pg C μm^{-3} for Peuk (Garrison et al., 2000). To derive an empirical equation relating cellular chlorophyll contents with normalized red fluorescence, we calculated cellular divinyl chlorophyll content of Pro by dividing divinyl chlorophyll concentrations measured by high performance liquid chromatography (HPLC) with corresponding Pro abundances. The relationship between cellular divinyl chlorophyll content of Pro and normalized red fluorescence could be well described by a log–log linear equation (Fig. 1B). We applied this relationship to approximately estimate cellular chlorophyll contents of Syn and Peuk because our main objective is not to compare chlorophyll-to-carbon ratios among groups but to compare the same group between seasons so that even deviations from real relationships between cellular chlorophyll content and normalized red fluorescence do not qualitatively affect the seasonal comparisons of

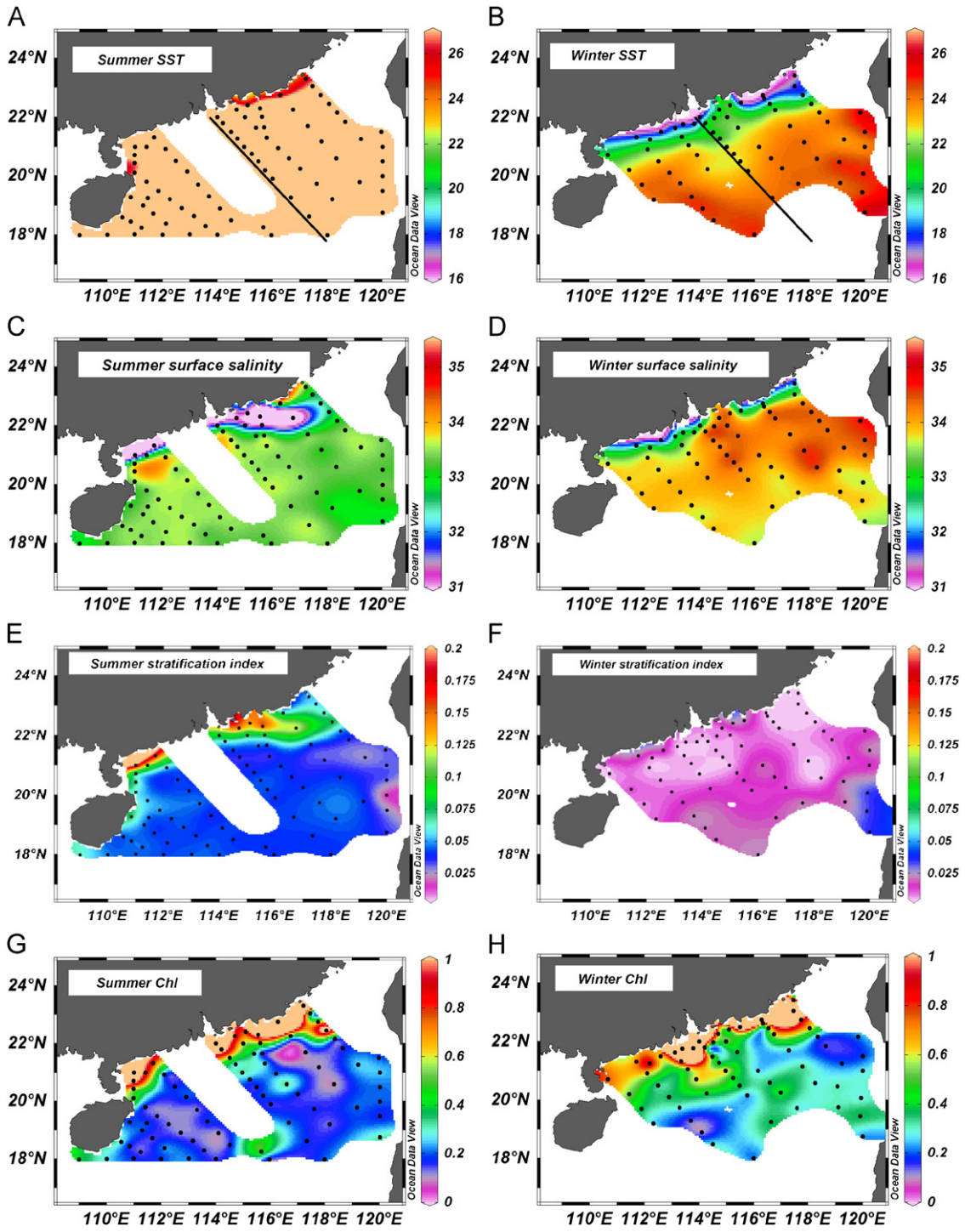

Fig. 2. Spatial distributions of (A,B) sea surface temperature (SST, °C), (C,D) sea surface salinity, (E,F) stratification index (kg m^{-4}), and (G,H) average Chl *a* concentrations (μg l^{-1}) over 0–150 m in summer and winter. The two black lines imposed on A and B represent Transect A.

chlorophyll-to-carbon ratios. The total carbon and chlorophyll biomass of picophytoplankton were estimated as the product of cellular carbon and chlorophll content and abundances.

Temperature, salinity, and pressure were determined by CTD probes. Seawater density was calculated from temperature, salinity, and pressure and stratification index was calculated as the density difference divided by depth difference between surface and bottom waters (or 100 m if the water depth is deeper than 100 m). Nitrate data was generously provided by M. Dai in Xiamen University, China, following standard methods (Parsons et al., 1984). The detection limit of nitrate was 0.1 μmol l^{-1}. The depth of nutricline was defined as the first depth where nitrate concentrations exceeded 1 μmol l^{-1}.

Chl *a* concentrations including monovinyl and divinyl Chl *a* were measured by HPLC according to the methods of Furuya et al. (1998). Four to sixteen liters of seawater were filtered onto 47 mm glass-fiber GF/F filters (Whatman) under low vacuum (<150 mmHg). The filters were frozen and stored in liquid nitrogen until analysis. Upon return to the lab, the filters were soaked in 2 ml N,N-dimethylformamide (DMF) at -20 °C for 2 h. The extractions were then filtered through 13 mm Whatman GF/F filters to clean the debris and mixed with ammonium acetate

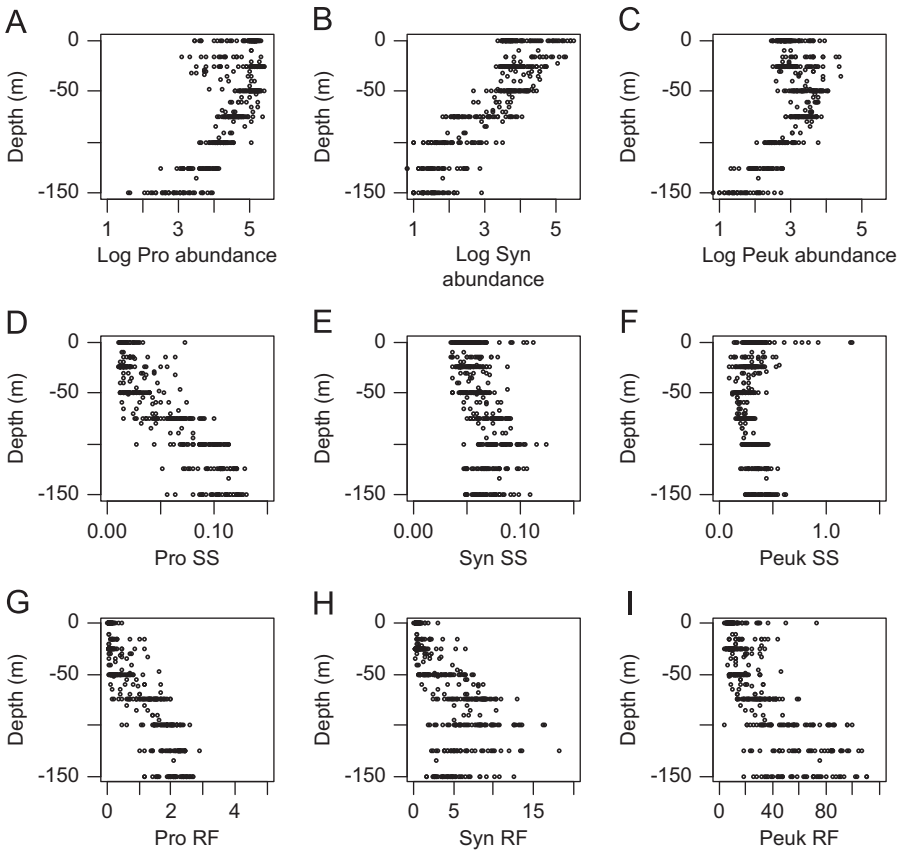

Fig. 3. Summer vertical distributions of (A–C) abundances (cells ml^{-1}), (D–F) normalized side-scattering (SS), and (G–I) normalized red fluorescence (RF) of *Prochlorococcus*, *Synechococcus*, and picoeukaryotes.

solution ($1\ mol\ l^{-1}$) at 1:1 ratio. Each mixture was partially injected into an Agilent series 1100 HPLC system fitted with a 3.5 μm Eclipse XDB C_8 column (100 mm × 4.6 mm; Agilent Technologies). Quantification was confirmed by the standards purchased from Danish Hydraulic Institute [DHI] Water and Environment, Hørsholm, Denmark. To calculate the standing stocks (Chl *a* concentrations and picophytoplankton abundances) of phytoplankton averaged over the epipelagic zone (top 150 m or the whole water column if the depth was shallower than 150 m), we first calculated the integrated standing stocks using a trapezoid rule and divided the integrated values by the water depth used in integration.

3. Results

3.1. Background of hydrology and chemistry

There was contrasting difference in physical background between summer and winter. Sea surface temperatures (SST) were relatively high (ranging from 25.3 to 30.5 °C with a median value 29.6 °C) during the summer, while SST were significantly lower (ranging from 16.2 to 25.9 °C with a median value 22.7 °C) during the winter (Wilcoxon rank test, $p < 0.001$). In both seasons, SST were usually lower in onshore than in offshore regions due to freshwater influence and coastal upwelling (Fig. 2A and B). The strong Pearl River freshwater discharge during the summer resulted in a prominent tongue with low surface salinity (< 32), extending near to 118°E, whereas the influence of Pearl River discharge was much weaker during the winter (Fig. 2C and D). Due to surface cooling in the winter, the upper 100 m water column was mostly homogeneously well mixed, and it was more stratified in the summer especially within the river plume (due to buoyancy of freshwater) and at some near-shore stations ($p < 0.001$; Fig. 2E and F). Surface salinities were also generally higher during the winter (median value = 33.87) than in the summer (median value = 33.42), indicating greater mixing in the winter ($p < 0.001$; Fig. 2C and D).

Due to greater stratification, surface nitrate concentrations were usually depleted during the summer (ranges = 0.02–3.89 $\mu mol\ l^{-1}$ with the median value = 0.11 $\mu mol\ l^{-1}$) except for a few coastal areas where freshwater discharge or coastal upwelling elevated nitrate concentrations (data courtesy of M. Dai in Xiamen University). Surface nitrate concentrations were much higher during the winter (ranges = 0.10–12.60 $\mu mol\ l^{-1}$ with the median value = 0.61 $\mu mol\ l^{-1}$; Wilcoxon rank test, $p < 0.001$), with generally higher values near the coast. Chl *a* concentrations (AChl) averaged over the epipelagic zone (top 150 m or the whole water column if the bottom depth is shallower than 150 m) were generally higher during the winter (ranges = 0.10–4.18 $\mu g\ l^{-1}$ with median value 0.40 $\mu g\ l^{-1}$) than in the summer (ranges = 0.09–3.72 $\mu g\ l^{-1}$ with median value 0.20 $\mu g\ l^{-1}$) ($p < 0.001$). Spatially, AChl showed pronounced onshore–offshore decreasing trends at both seasons (Fig. 2G and H; Spearman rank correlation coefficient $r_s = -0.62$ and -0.85 for the correlations between station bottom depth and AChl in the summer and winter, respectively, $p < 0.001$).

3.2. Vertical distribution of picophytoplankton abundances and biomass

We plot all the data points of picophytoplankton abundance, SS, and RF against depth in Figs. 3 and 4 to see a general vertical pattern. We also select one transect (Transect A) extending from Pearl River estuary to the deep basin (Figs. 5–7) as an example to

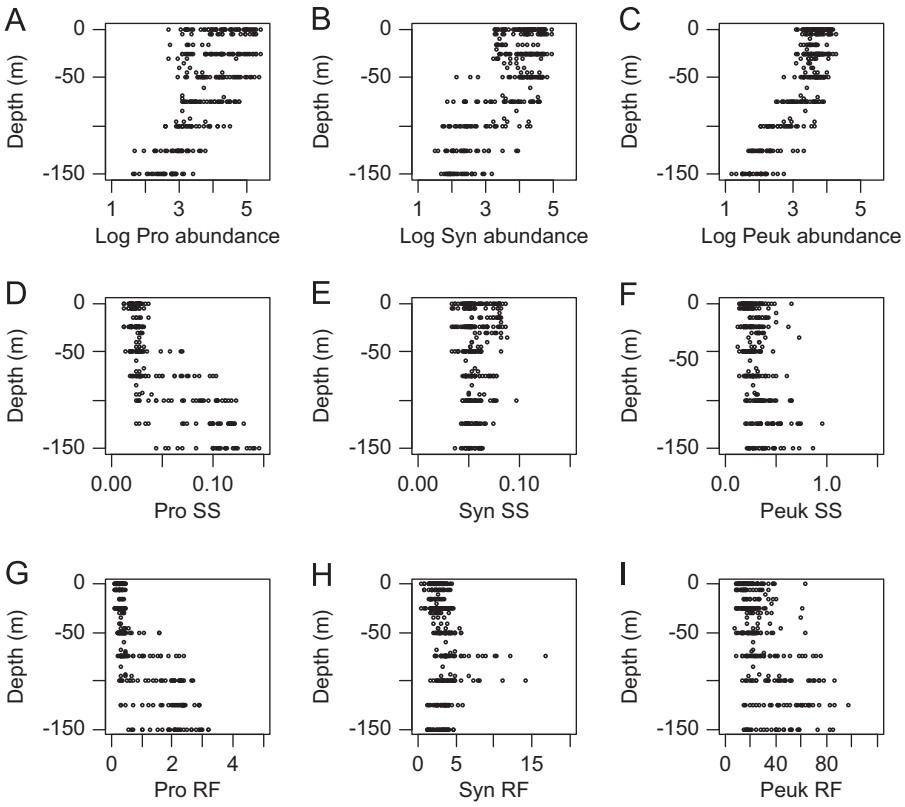

Fig. 4. The same as Fig. 3, but for winter data.

show the onshore–offshore gradients of picophytoplankton abundance, single-cell properties, and biomass. Vertically, the abundance of Peuk usually exhibited a subsurface maxima around 50 or 75 m, similar to the vertical distribution of total Chl *a* (Figs. 3C and 5), while the vertical distribution of Peuk abundance was more homogeneous in the surface mixed layer during the winter (Figs. 4C and 5). In the upper mixed layer, Pro abundances were significantly higher in the summer than in the winter throughout the majority of the transect (Table 1; Fig. 5A and B). During the summer, Pro abundances showed two peaks along the onshore–offshore transect, one located at the station with 70 m bottom depth and the other beyond the continental slope. During the winter, Pro abundances were the greatest at the southern offshore end of the transect. In contrast, surface Syn and Peuk abundances were usually higher in the winter than in the summer (Table 1; Figs. 3B and C, 4B and C, and 5C–F). During the summer, Syn abundances were highest at near-shore waters, while the maximal Syn and Peuk abundances during the winter occurred at stations deeper than 50 m. The vertical distributions of Peuk abundances were similar with those of Chl *a* concentrations, which was confirmed by the close associations between Peuk abundances and Chl *a* concentrations (Spearman $r_s=0.82$, $p \ll 0.001$). The depth of maximal abundances of Peuk was positively rank correlated with nutricline depth during the summer ($r_s=0.58$, $p \ll 0.001$, $n=59$) for stations deeper than 50 m.

In contrast to the decreasing vertical gradients of abundances of Pro and Syn from surface to deep waters ($r_s=-0.32$ and –0.71 for the correlations between abundance and depth of Pro and Syn, respectively, $p<0.001$), cellular SS and RF usually increased from surface to deep layers ($r_s=0.81$ and 0.31 for the correlation between SS and depth of Pro and Syn, respectively, and $r_s=0.83$ and 0.63 for the correlation between RF and depth of Pro and Syn, respectively, $p<0.001$ in all cases; Figs. 3, 4, and 6). Notably, Peuk showed minimum SS at depths with maximal abundances during the summer (Figs. 3F and 6E), suggesting that high abundances of Peuk at subsurface maximum were due to increases of small Peuk cells. However, a similar trend was not observed for RF of Peuk at the same time (Fig. 3I), suggesting that the increase of fluorescence with depth counteracted the decreased SS at subsurface maximum layers. In surface waters, SS of both Pro and Syn were significantly larger in the winter than in the summer, while SS of Peuk were smaller in the winter (Table 1). RFs and chlorophyll-to-carbon ratios of all three picophytoplankton groups in surface waters were significantly higher in the winter than in the summer (Table 1).

As a result of the increased cell size and cellular pigment content in deep waters, all three picophytoplankton groups exhibited subsurface maximum of carbon and Chl *a* contents at most summer stations, while the carbon and Chl *a* contents of picophytoplankton groups were uniformly distributed in surface mixed layers during the winter (carbon data shown in Fig. 7). The distributions of the sum of the carbon and Chl *a* contents of three picophytoplankton groups were qualitatively similar with those of Chl *a* concentrations measured by HPLC.

3.3. Spatial distributions of picophytoplankton abundances and biomass

Pro abundances averaged over top 150 m after integration using a trapezoid rule (APro) usually increased from onshore to offshore waters ($r_s=0.28$ and 0.80 for the correlation between APro and bottom depth of summer and winter, respectively, $p<0.05$; Fig. 8). The maximal APro was found roughly along the 80–100 m isobath during the summer. During the winter, APro were much less abundant than in the summer (Table 1) and were absent at many near-shore sites, showing clear onshore–offshore increasing trends. Median APro decreased about 10-folds in the winter compared to the summer (Table 1). In the pooled data set, APro were positively rank correlated with nutricline depth ($r_s=0.59$, $p \ll 0.001$).

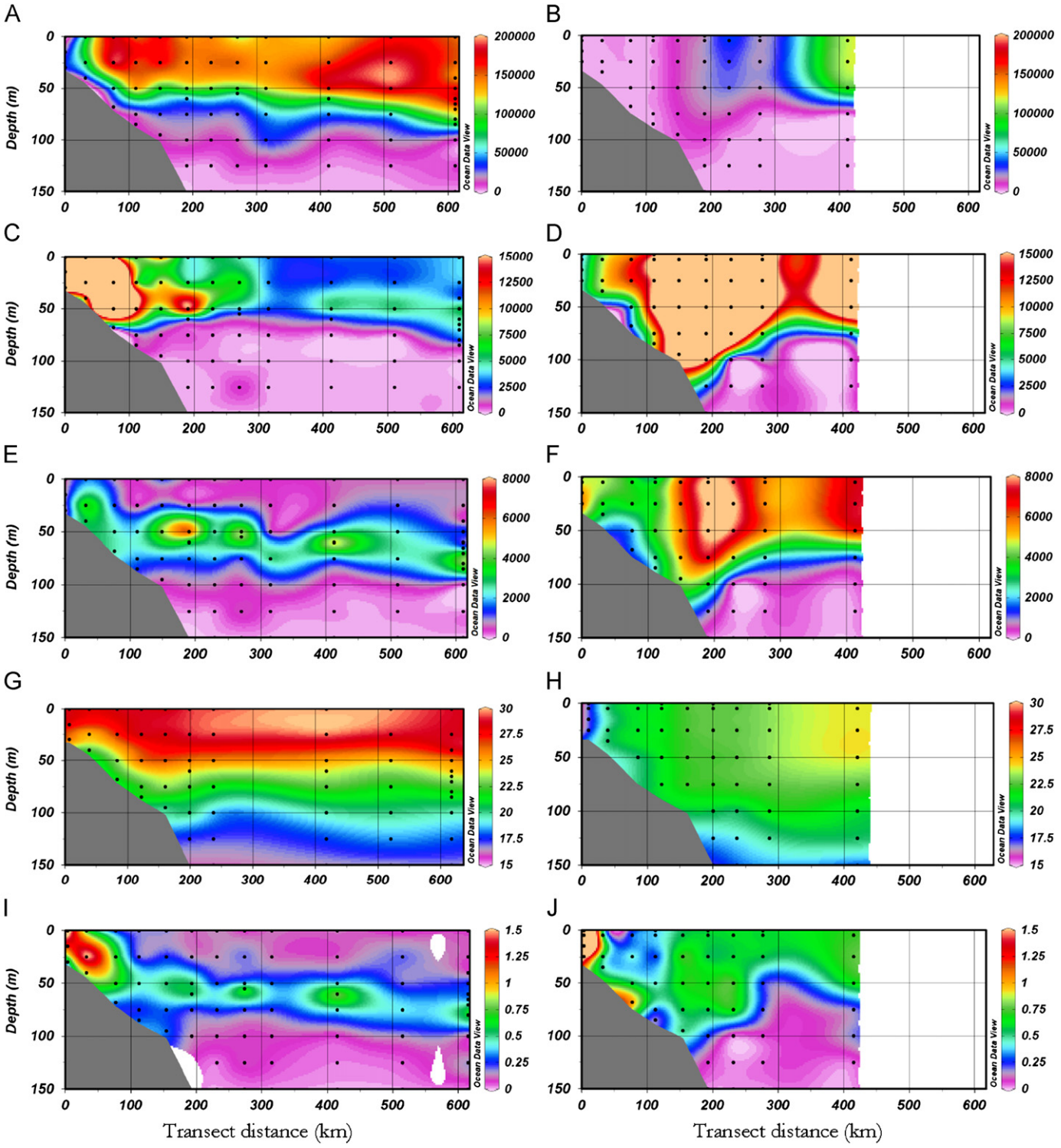

Fig. 5. Distributions of (A,B) *Prochlorococcus* abundances (cells ml^{-1}), (C,D) *Synechococcus* abundances, (E,F) picoeukaryote abundances, (G,H) temperature (°C), and (I,J) Chl *a* concentrations ($\mu g\ l^{-1}$) along Transect A. (A) Summer Pro abundance, (B) Winter Pro abundance, (C) Summer Syn abundance, (D) Winter Syn abundance, (E) Summer Peuk abundance, (F) Winter Peuk abundance, (G) Summer temperature, (H) Winter temperature, (I) Summer Chl a and (J) Winter Chl a.

Syn and Peuk abundances averaged over top 150 m (ASyn and Apeuk) were higher near the coast than offshore during the summer ($r_s = -0.71$ and -0.52 for the correlations between averaged abundances and bottom depth of Syn and Peuk, respectively, $p < 0.001$ in the summer; Fig. 8). ASyn were significantly negatively correlated with surface salinity ($r_s = -0.33$, $p < 0.01$), indicating the effect of the Pearl River plume on ASyn (Fig. 8). During the winter, however, there were no apparent onshore–offshore decreasing trends of ASyn and Apeuk ($p > 0.05$ for the correlations between averaged abundances and bottom depth of both Syn and Peuk in the winter; Fig. 8). Both ASyn and Apeuk were lower at very near-shore sites, especially during the winter (Fig. 8). Median ASyn and Apeuk increased 2.6 and 2.4 times, respectively, in the winter (Table 1). Three water masses with elevated ASyn and Apeuk were seen during the winter (Fig. 8D and F). One covered from 111°E to 116°E and 20°N to 21°N. Another

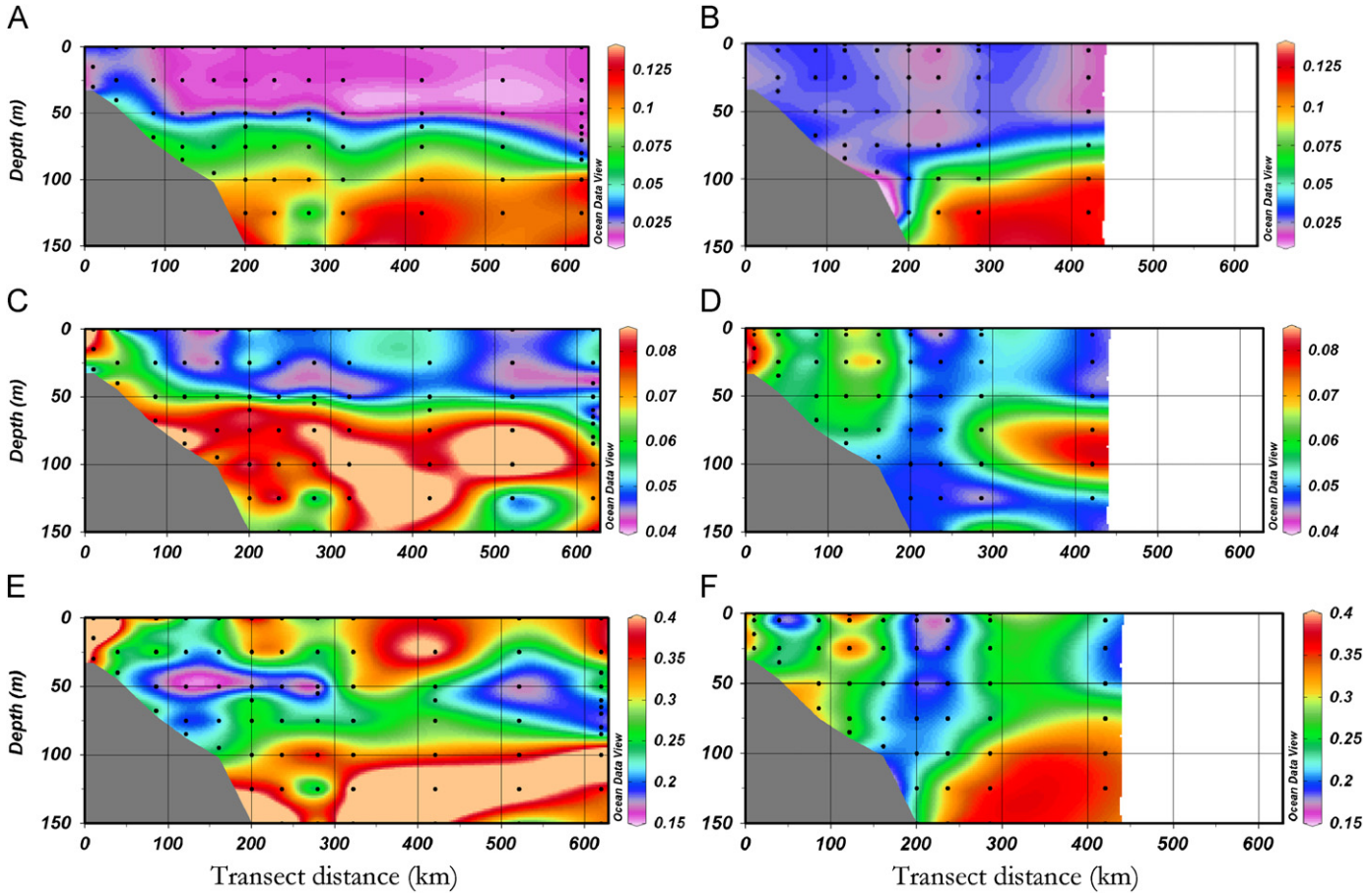

Fig. 6. Distributions of normalized side scattering (SS) of (A,B) *Prochlorococcus*, (C,D) *Synechococcus*, and (E,F) picoeukaryotes along Transect A. (A) Summer Pro SS, (B) Winter Pro SS, (C) Summer Syn SS, (D) Winter Syn SS, (E) Summer Peuk SS and (F) Winter Peuk SS.

extended from the Pearl River estuary to the east until 119°E. The third was rather offshore, covering from 117°E to 120°E and from 19°N to 21°N. The similarity in the distributions of ASyn and Apeuk was confirmed by the highly positive correlations between ASyn and Apeuk in both seasons (r_s=0.60 and 0.55 for summer and winter, respectively, $p \ll 0.001$). In the pooled data set, Apeuk, but not ASyn, was negatively rank correlated with nutricline depth ($r_s=-0.32$, $p<0.001$). The distributions of carbon and Chl *a* contents of three picophytoplankton groups averaged over top 150 m were similar with those of abundances (the carbon data are shown in Fig. 9, the Chl *a* data are similar with carbon data). Carbon and Chl *a* contents of Syn, Peuk, and the sum of the three groups were highest near the coast during the summer, particularly within areas affected by the Pearl River plume where average Peuk sizes were large, while the carbon and Chl *a* contents of Syn, Peuk, and the sum of the three picophytoplankton groups were highest in the western parts of the studied area during the winter.

The relationships between picophytoplankton abundances averaged over top 150 m and environmental variables (sea surface temperature (SST), nitrate concentrations (S_{NO_3}), and Chl *a* concentrations averaged over top 150 m) are shown in Fig. 10. APro increased monotonically with SST (r_s=0.30 and 0.91 for summer and winter, respectively, $p<0.01$) and decreased with S_{NO_3} ($r_s=-0.21$ and -0.54 for summer and winter, respectively, $p<0.01$ for winter) and Chl *a* ($r_s=-0.31$ and -0.76 for summer and winter, respectively, $p<0.01$) in both summer and winter. ASyn and Apeuk showed maximal values at intermediate SST, S_{NO_3}, and Chl *a*. The optimal SST of ASyn and Apeuk was, however, different for summer (approximately 27.5 °C for both ASyn and APeuk) and winter (approximately 23 °C). The differences in the optimal S_{NO_3} of ASyn and APeuk (around $10^{-0.4}$=0.4 μmol l^{-1}) between summer and winter were much less remarkable. The optimal Chl *a* of ASyn was around $10^{0.2}$=1.6 μg l^{-1} in the summer and roughly $10^{-0.2}$=0.63 μg l^{-1} in the winter. The optimal Chl *a* of Apeuk was also roughly 0.6 μg l^{-1} in both seasons.

To investigate the spatial environmental effects on cell-specific size and fluorescence, we focus on the environmental correlates of surface (5 m) size and fluorescence of picophytoplankton cells, which presumably grow under light-saturated conditions. A common pattern is that nitrate concentrations were positively correlated with RF of all three groups of picophytoplankton on the surface waters (r_s=0.67, 0.59, and 0.64, for Pro, Syn, and Peuk, respectively, $p<0.01$). Nitrate concentrations were also positively correlated with SS of Pro and Syn in surface waters (r_s=0.56 and 0.36 for Pro and Syn, respectively, $p<0.01$), but not of Peuk ($p>0.01$). Temperature, on the contrary, was negatively correlated with RF of all three groups of picophytoplankton on the surface waters ($r_s=-0.77$, -0.78, and -0.63, for Pro, Syn, and Peuk, respectively, $p<0.01$). Temperature was also negatively correlated with SS of Pro and Syn ($r_s=-0.56$ and -0.19 for Pro and Syn, respectively, $p<0.05$), but was positively correlated with SS of Peuk (r_s=0.34, $p<0.01$).

4. Discussion

4.1. Environmental controls on picophytoplankton cell size

One of the uncertainties in the estimation of phytoplankton biomass is the quantification of cell size or cellular carbon content

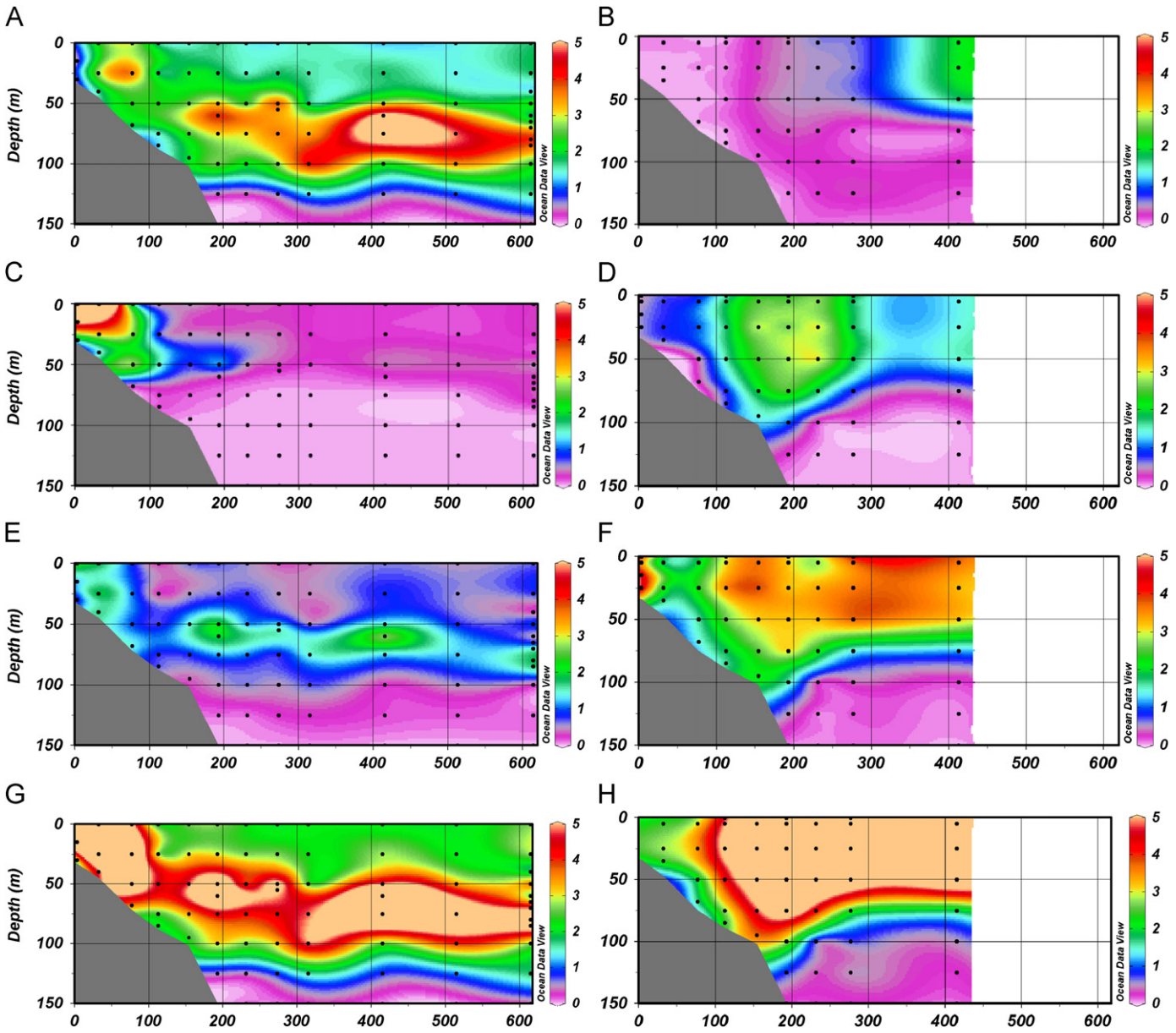

Fig. 7. Vertical distributions of carbon contents ($\mu g\ C\ l^{-1}$) of (A,B) *Prochlorococcus*, (C,D) *Synechococcus*, (E,F) picoeukaryotes, and (G,H) total ultraphytoplankton along Transect A. (A) Summer Pro carbon, (B) Winter Pro carbon, (C) Summer Syn carbon, (D) Winter Syn carbon, (E) Summer Peuk carbon, (F) Winter Peuk carbon, (G) Summer ultraphythoplankton carbon and (H) Winter ultraphythoplankton carbon.

(Zubkov et al., 1998). Some previous studies used fixed conversion factors (53 fg C $cell^{-1}$ for Pro and 250 fg C $cell^{-1}$ for Syn reported by Campbell et al. (1994), 32 fg C $cell^{-1}$ for Pro and 103 fg C $cell^{-1}$ for Syn reported by Zubkov et al. (1998), 24 fg C $cell^{-1}$ for Pro and 67 fg C $cell^{-1}$ for Syn above 60 m and 62 fg C $cell^{-1}$ for Pro and 157 fg C $cell^{-1}$ for Syn below 60 m reported by Liu et al. (2007)), which might not be suitable for a vast area comprising different geographic provinces. The empirically determined relationship between SS and cell volume using phytoplankton cultures, which is better than calibration based on artificial latex beads, can provide more accurate estimates for picophytoplankton biomass (Durand et al., 2001; Worden et al., 2004; Bec et al., 2008). The values of cellular carbon contents we obtained are at the lower end of literature reports, but are comparable with the estimates by Liu et al. (2007) at the SEATS stations in the South China Sea basin (Note that Table 1 only shows surface values, which are usually lower than that of deeper waters).

Environmental variables usually have pronounced effects on phytoplankton size (Chisholm, 1992; Finkel et al., 2007, 2009). Phytoplankton size usually increases with nutrient availability in marine systems for mixed phytoplankton assemblages, suggestive of a community succession from small to large species with increasing productivity (Chisholm, 1992; Li, 2002; Finkel et al., 2007; Chen and Liu, 2010), but environmental controls on sizes of one particular phytoplankton group have been less often investigated in the ocean. Vertically, cell size of Pro and Syn increased with depth especially during the summer when water column stratified (Fig. 3). Spatially, for cells from surface mixed layers, cell sizes of Pro and Syn were also larger at onshore regions and in the winter with higher ambient nutrient concentrations (Fig. 6). These patterns appear widespread in the field observations. For example, Pro cells in the oligotrophic western Pacific were smaller than in the eastern high nitrate low chlorophyll (HNLC) eastern Pacific (Blanchot et al., 2001).

Table 1
Comparisons of median abundances (10^3 cells ml^{-1}), cellular carbon and Chl *a* contents (fg $cell^{-1}$), community carbon and Chl *a* contents of *Prochlorococcus* (Pro), *Synechococcus* (Syn), and picoeukaryotes (Peuk) between summer and winter. The numbers in parenthesis indicate minimal and maximal values. Cellular Chl *a* contents of Pro were directly estimated from divinyl Chl *a* concentrations measured by HPLC, while cellular Chl *a* contents of Syn and Peuk were estimated using the equation in Fig. 1B. Surface = 5 m. The stars adjacent to the winter data values represent the significance of comparisons between the two seasons (Wilcoxon rank test). *: $p < 0.05$, **: $p < 0.01$.

	Prochlorococcus		*Synechococcus*		Picoeukaryotes	
	Summer	Winter	Summer	Winter	Summer	Winter
Surface abundance	118.9 (0–210.2)	11.6** (0–256.0)	6.1 (2.5–317.1)	20.5 (1.8–92.0)	0.7 (0.3–8.8)	5.2** (1.3–15.7)
Surface cellular carbon	11.8 (7.3–124.0)	23.4** (8.3–44.7)	72.4 (41.2–238.8)	76.7* (39.4–161.3)	979.1 (258.7–6918.8)	580.7** (258.7–2588.2)
Surface cellular Chl	0.28 (0.07–1.42)	0.97** (0.06–1.65)	1.04 (0.51–3.57)	3.12** (1.05–4.60)	6.80 (4.55–26.54)	10.64** (6.85–24.39)
Surface Chl:C	0.024 (0.001–0.063)	0.045** (0.008–0.070)	0.014 (0.004–0.037)	0.041** (0.016–0.074)	0.007 (0.003–0.025)	0.019** (0.009–0.026)
Averaged abundance[a]	70.5 (0–174.1)	7.2** (0–98.1)	4.3 (1.2–138.1)	11.3** (1.6–72.5)	1.6 (0.5–18.4)	3.8** (1.3–10.3)
Averaged community carbon[b]	2.13 (0.08–3.56)	0.34** (0–2.46)	0.33 (0.08–14.11)	0.81** (0.12–5.26)	1.21 (0.57–10.45)	2.91** (1.04–8.13)

[a] Abundances averaged over 0–150 m after integration using a trapezoid rule (*see* the section "Methods"). *Units*: 10^3 cells ml^{-1}.
[b] Community carbon contents averaged over 0–150 m after integration using a trapezoid rule. *Units*: $\mu g\ C\ l^{-1}$.

The above patterns could be the results of the effects of low-light, high-nutrient concentration, and/or low temperature on phytoplankton size within species, and could also result from changes in the dominance of different ecotypes with different sizes. Pro cells are well known for consisting of two distinct ecotypes inhabiting high-light and low-light environments, with low-light ecotypes being larger, which could sometimes be observed from the cytograms (Moore et al., 1998; Zubkov et al., 1998; Blanchot et al., 2001). The high diversity of Syn and Peuk is also often reported in the literature (Jing et al., 2009, 2010). Distinguishing one causal factor from others simply from field observations is confounded by the correlative nature of these environmental parameters. Inference from lab experiments could help in understanding the causal effects of the various factors on phytoplankton size.

The hypothesis that higher ambient nutrient concentrations induce larger size within a species is not supported by data from lab cultures. Liu et al. (1999) observed that the cell size of *Synechococcus* WH7803 was larger in more nitrate-limiting chemostat cultures. Bertilsson et al. (2003) reported that cellular carbon contents and forward light scatterings of one *Prochlorococcus* strain (MED4) and two *Synechococcus* strains (WH8103 and WH8012) increased in phosphorus-starved batch cultures. It is conceivable that, under nutrient-limiting conditions, phytoplankton cell division is delayed due to the lack of limiting nutrient elements but phytoplankton size increases for storage of carbon. An alternative hypothesis for the larger size in less oligotrophic waters is that size might be larger under lower light because of the need to synthesize more proteins and pigments to capture limiting photons. Package effects are negligible in such small cells so that increase in size will not reduce the efficiency of light harvesting (Morel et al., 1993; Raven, 1998). Lab results on the light-size relationships are mixed. Burbage and Binder (2007) found that cell sizes of oceanic *Prochlorococcus* MIT9312 and *Synechococcus* WH8103 increased at low light in light-limited semi-continuous cultures, in which the light availability controls the growth rate of *Synechococcus*. However, Binder and Liu (1998) found that the coastal strain *Synechococcus* WH8101 increased biovolume under relatively high light also in light-limited semi-continuous cultures. Hence, it is still uncertain whether the size differences in oligotrophic versus mesotrophic waters can be attributed to light effects. Lower temperature in nutrient-richer environments could also lead to larger size (known as the Bergmann's rule), with roughly 4% increase of cell volume per °C decrease (Montagnes and Franklin, 2001). In our data set, the absolute slope of cell volume against temperature ($\mu m^3\ °C^{-1}$) divided by median cell volume (μm^3) is 0.67, 0.047, and 0.041 for Pro, Syn, and Peuk, respectively, suggesting that the size-temperature relationships of Syn and Peuk, but not of Pro, appear similar with those of diatoms. It is probable that changes in phytoplankton composition, at least for Pro, are critical in explaining the variations in picophytoplankton size.

4.2. Distributions of picophytoplankton abundance are related with their physiology

Responses of major groups of picophytoplankton to environmental forcing are in accordance with previously documented physiology of picophytoplankton and are consistent with reports from other seas. Pro cells have been shown to prefer high temperature, low nutrient, and stratified water column, while Syn and Peuk cells are able to tolerate lower temperatures and are most abundant under conditions with intermediate nutrient concentrations and mixed water column (Moore et al., 1995; Campbell et al., 1997; Liu et al., 1998; Zubkov et al., 1998; Agawin et al., 2000). It is usually believed that Pro cells have lost the

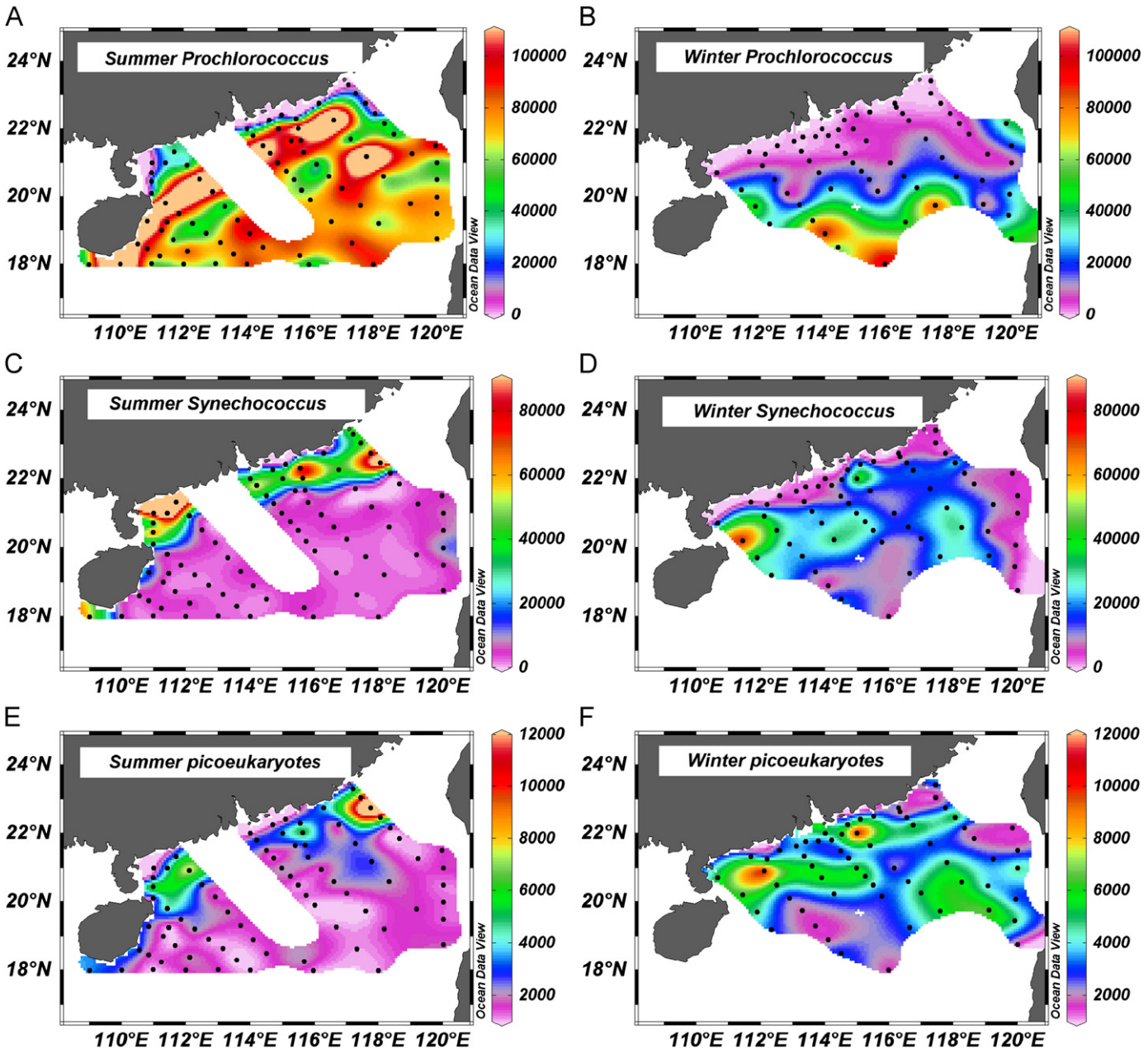

Fig. 8. Spatial distributions of abundances (cells ml^{-1}) of (A,B) *Prochlorococcus*, (C,D) *Synechococcus*, and (E,F) picoeukaryotes averaged over 0–150 m during summer and winter.

capability to utilize nitrate (Moore et al., 2002; Rocap et al., 2003, but see Casey et al., 2007) and elevated concentrations of nutrients and heavy metals could be toxic to them (Mann et al., 2002; Worden and Binder, 2003) so that Pro abundances decreased at near-shore regions where other larger phytoplankton could benefit from increased nutrient availability. The large decrease of Pro abundances in the winter could be a combined result of low temperature, 'toxic' effects of high concentrations of nutrients and heavy metals partially delivered by northeastern monsoons via atmospheric deposition, limited ability of chromatic adaptation to frequent mixing events, and inferior ability to absorb green light in high chlorophyll waters due to winter mixing (Bouman et al., 2006; Johnson et al., 2006).

With slightly larger size and different pigment contents, Syn has distinct distributional patterns and physiological traits with Pro (Rocap et al., 2003). In subtropical and tropical oceans, Syn was usually most abundant during the winter, sometimes leading to a winter 'bloom' (Olson et al., 1990; Campbell et al., 1997; Liu et al., 2007), while in temperate or some coastal waters, Syn usually bloomed during the summer (Waterbury et al., 1986; Agawin et al., 1998; Liu et al., 2002a; Chen et al., 2009). Along the Atlantic meridional transect, Syn showed peak abundances around 40–50° in two hemispheres except in the tropical region affected by the Mauritanian upwelling where Syn abundances increased (Zubkov et al., 1998, 2000). Agawin et al. (2000) experimentally showed that the growth of Syn was optimal at nitrogen concentrations of 0.25 $\mu mol\ l^{-1}$ (which is comparable with the optimal nitrate concentration of 0.4 $\mu mol\ l^{-1}$ for ASyn in our data set), while higher concentrations of nitrogen could inhibit Syn growth. While growth rates of Syn usually increase linearly with temperature and low temperature directly constrains Syn growth (Agawin et al., 1998; Li, 1998), low nutrient concentrations limit the growth of Syn in the oligotrophic open ocean at high temperatures since temperature and nutrient

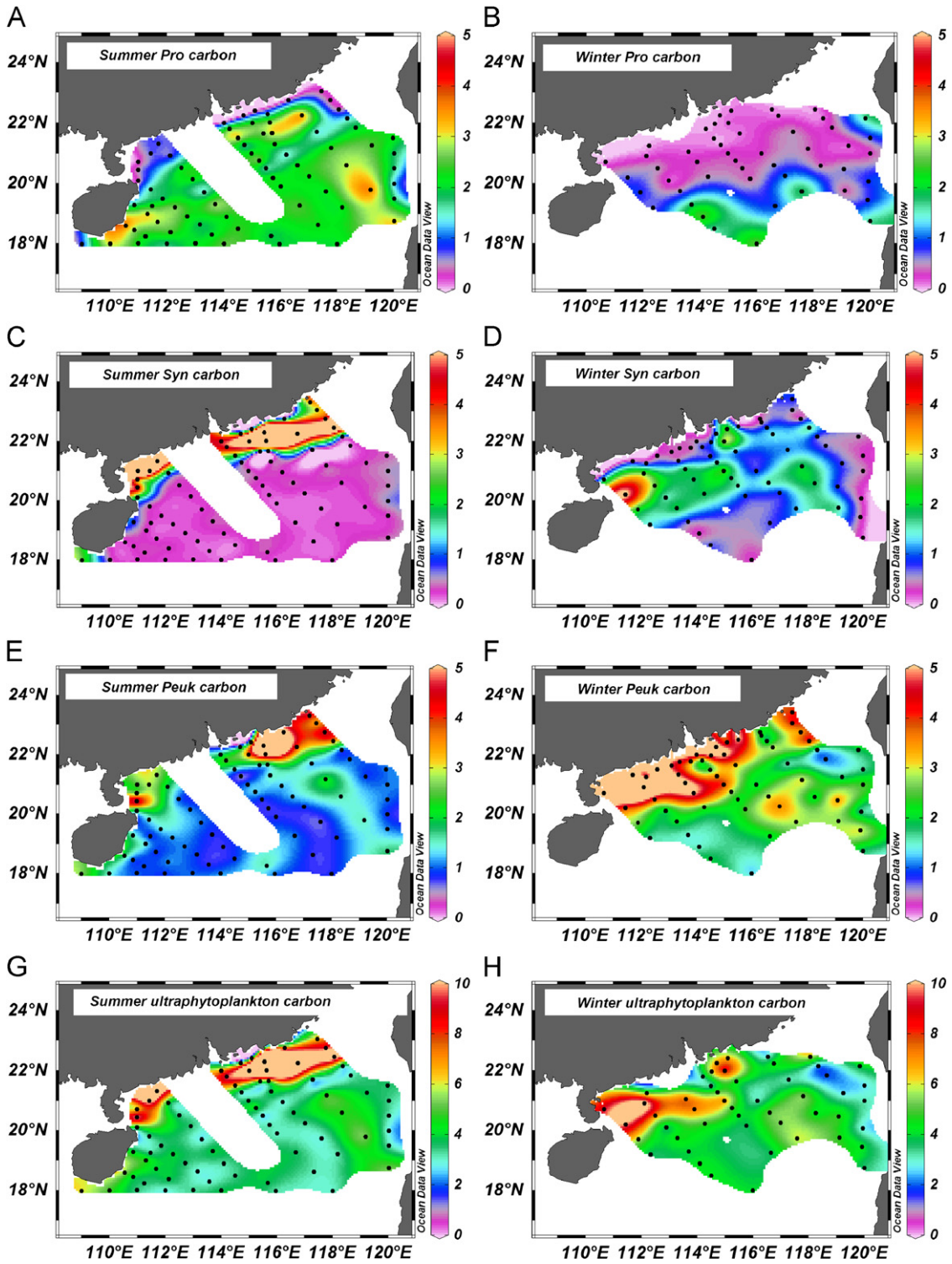

Fig. 9. Spatial distributions of carbon contents ($\mu g\, l^{-1}$) of (A,B) *Prochlorococcus*, (C,D) *Synechococcus*, (E,F) picoeukaryotes, and (G,H) total ultraphytoplankton averaged over 0–150 m during summer and winter.

concentrations are usually negatively correlated (Li, 1998). Mesotrophic waters with intermediate chlorophyll concentrations led to a green-light environment, which favors the light harvesting by Syn possessing phycobiliproteins (Bouman et al., 2006). As such, it is not surprising to find maximal Syn abundances at intermediate temperature, nutrient and chlorophyll concentrations, which is exactly the case in our observations (Fig. 10).

Peuk cells seem to share similar niches with Syn in terms of optimal temperature and nutrient concentrations, although the dependence of their growth on temperature, in general, should be weaker than that of prokaryotes (Paerl and Huisman, 2008). Maximal abundances of Peuk also occurred at intermediate temperature, nutrient and chlorophyll concentrations (Fig. 10). The high diversity of Peuk might render them less variability of abundances across different environments.

As a result of different physiological preferences in different picophytoplankton groups, we have observed differential responses of the three groups to the same changes in physical

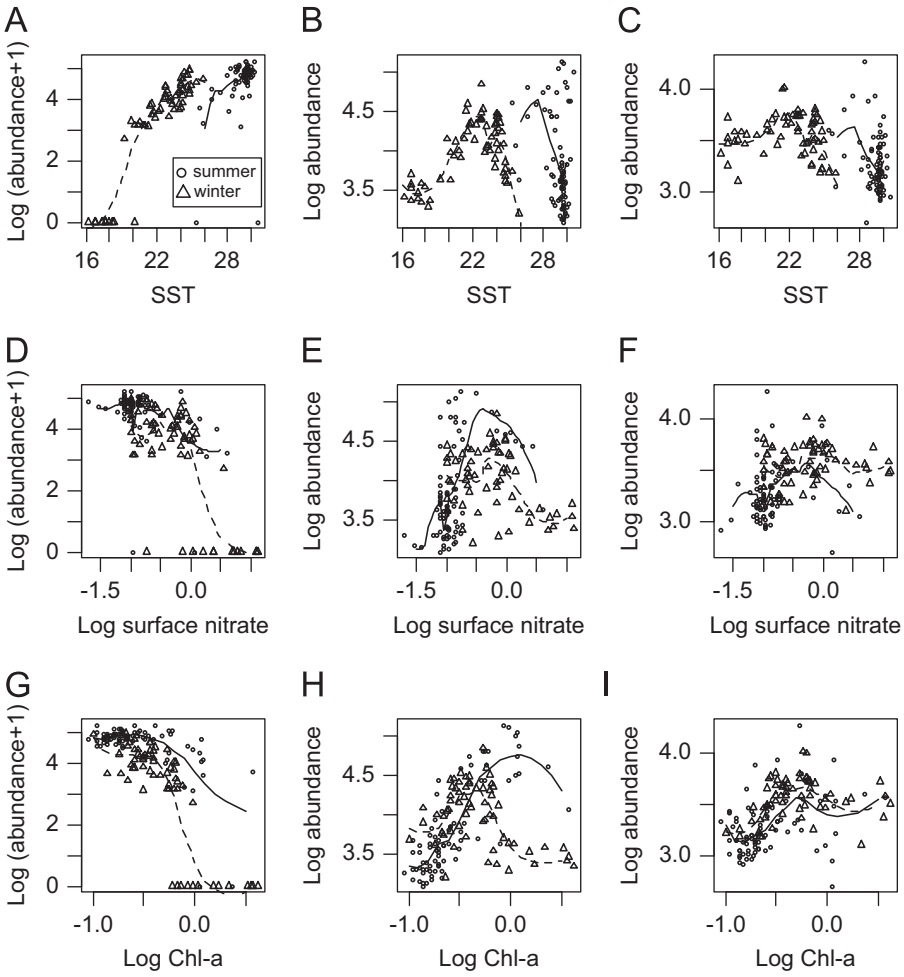

Fig. 10. Scatter plots of $\log_{10}$ abundances (cells ml^{-1}) against (A–C) sea surface temperature (SST, °C), (D–F) $\log_{10}$ surface nitrate concentrations (μmol l^{-1}), and (G–I) $\log_{10}$ Chl *a* concentrations (μg l^{-1}) averaged over 0–150 m. Solid and dashed lines represent local polynomial regression (loess) fitting lines for summer and winter, respectively. (A) Pro, (B) Syn, (C) Peuk, (D) Pro, (E) Syn, (F) Peuk, (G) Pro, (H) Syn and (I) Peuk.

and chemical environments. Owing to the preference of Pro cells for high temperature and low nutrients, which is distinctly different from those of other larger phytoplankton, the responses of Pro abundances differed from those of total Chl *a*, Syn, and Peuk cells. Pro abundances decreased dramatically during the winter compared with the summer, while total Chl *a* concentrations and abundances of Syn and Peuk cells increased during the winter. On the contrary, the responses of cell size and fluorescence of different groups were similar, suggesting common underlying physiological mechanisms. For example, the Bergmann's rule (i.e., size decreases with increasing temperature) might apply similarly to Pro, Syn, and Peuk cells within a species, which could be further validated by lab experiments. The increase of cellular fluorescence/pigment to the increases in nutrient supply is also a robust pattern in all phytoplankton groups, reinforcing the notion that nutrients (presumably nitrogen) are essential in maintaining the photosynthetical capacity of all phytoplankton groups including Pro, but are not necessary in biomass accumulation.

The close associations between physiological features and biogeographic distributions suggest that the algal physiology and phytoplankton biogeography should be linked tightly to gain deeper understanding on the population dynamics of phytoplankton in the ocean. Mechanistic models combining physiological characteristics of phytoplankton and global ocean circulation models have been successfully constructed to simulate the global biogeographic distributions of phytoplankton including different ecotypes of Pro and Syn (Follows et al., 2007). Similar exercises can be conducted in regional scales with higher spatial resolution. It is also possible to build statistical models using physical parameters to predict standing stocks of phytoplankton without *a priori* specifications of particular functional terms describing growth and death (Irwin and Finkel, 2008). Equipped with appropriate models, we might be able to strengthen our ability to predict the responses of phytoplankton to future climate change.

4.3. Geochemical implications of changes in phytoplankton community structure

The changes in picophytoplankton community structure have important implications for nutrient cycles and food web dynamics. For example, Pro cells in surface waters are usually considered to be unable to take up nitrate but can take up considerable amounts of organic nitrogen (Moore et al., 2002; Zubkov et al., 2003). It has also been observed that Pro cells may be less subject to protistan grazing and viral infection than Syn (Christaki et al., 1999; Sullivan et al., 2003). Therefore, the observed large decrease of Pro abundance during the winter would have a great impact on the seasonal nitrogen cycle and food web dynamics, which cannot be deduced from changes in bulk Chl *a* concentrations alone. Appreciable amounts of organic nitrogen can be directly assimilated by Pro instead of strictly heterotrophic bacteria during the summer, directly fueling primary production and increasing nitrogen recycling rate.

The increased cellular pigment content related with increased cellular nitrogen quota in picophytoplankton cells during the winter may also suggest that they were of greater nutritional value to protistan grazers. However, the low temperature during the winter might limit the feeding rates of micro- and mesozooplankton (Chen et al., unpublished data), counterbalancing the effect of improved prey nutritional quality in increasing trophic transfer efficiencies. The responses of phytoplankton community structure, nutritional value, and food web dynamics to the changing physical and chemical backgrounds should deserve further investigation.

Acknowledgments

This study was supported by the National Basic Research Program ("973" Program) of China through Grant 2009CB421203, Hong Kong University Grant Council through the Area of Excellence program (AoE/P-04/04) and Research Grant Council General Research Fund Grants (661407 and 661809) provided to H.L., National Science Foundation of China Grant (NSFC 40730846) provided to B.H., and National Science Foundation of China Grant (NSFC 90711006) and Chinese Academy of Sciences grant (KZCX2-YW-QN205) provided to J.S. We sincerely thank the captain and crew of the research vessel *Dongfanghong2* and the chief scientists Minhan Dai, Pinghe Cai, and Weidong Zhai for organizing the cruises. We also thank Jianyu Hu, Jia Zhu, and Zhenyu Sun for providing the CTD data and Yong Zhang, Yanping Xu, and Lifang Wang for providing the nutrient data.

References

Agawin, N.S.R., Duarte, C.M., Agustí, S., 1998. Growth and abundance of *Synechococcus* sp. in a Mediterranean Bay: seasonality and relationship with temperature. Mar. Ecol. Prog. Ser. 170, 45–53.

Agawin, N.S.R., Duarte, C.M., Agustí, S., 2000. Response of Mediterranean *Synechococcus* growth and loss rates to experimental nutrient inputs. Mar. Ecol. Prog. Ser. 206, 97–106.

Bec, B., Collos, Y., Vaquer, A., Mouillot, D., Souchu, P., 2008. Growth rate peaks at intermediate cell size in marine photosynthetic picoeukaryotes. Limnol. Oceanogr. 53, 863–867.

Bertilsson, S., Berglund, O., Karl, D.M., Chisholm, S.W., 2003. Elemental composition of marine *Prochlorococcus* and *Synechococcus*: implications for the ecological stoichiometry of the sea. Limnol. Oceanogr. 48, 1721–1731.

Binder, B.J., Liu, Y.C., 1998. Growth rate regulation of rRNA content of a marine *Synechococcus* (Cyanobacterium) strain. Appl. Environ. Microbiol. 64, 3346–3351.

Blanchot, J., André, J.-M., Navarette, C., Neveux, J., Radenac, M.-H., 2001. Picophytoplankton in the equatorial Pacific: vertical distribution in the warm pool and in the high nutrient low chlorophyll conditions. Deep-Sea Res. I 48, 297–314.

Bouman, H.A., et al., 2006. Oceanographic basis of the global surface distribution of *Prochlorococcus* ecotypes. Science 312, 918–921.

Burbage, C.D., Binder, B.J., 2007. Relationship between cell cycle and light-limited growth rate in oceanic *Prochlorococcus* (MIT9312) and *Synechococcus* (WH8103) (cyanobacteria). J. Phycol. 43, 266–274.

Campbell, L., Liu, H.B., Nolla, H.A., Vaulot, D., 1997. Annual variability of phytoplankton and bacteria in the subtropical North Pacific Ocean at Station ALOHA during the 1991–1994 ENSO event. Deep-Sea Res. I 44, 167–192.

Campbell, L., Nolla, H.A., Vaulot, D., 1994. The importance of *Prochlorococcus* to community structure in the central North Pacific-Ocean. Limnol. Oceanogr. 39, 954–961.

Casey, J.R., Lomas, S.W., Mandecki, J., Walker, D.E., 2007. *Prochlorococcus* contributes to new production in the Sargasso Sea deep chlorophyll maximum. Geophys. Res. Lett. 34, L10604. doi:10.1029/2006GL028725.

Chen, B.Z., Liu, H.B., 2010. Relationships between phytoplankton growth and cell size in surface oceans: Interactive effects of temperature, nutrients, and grazing. Limnol. Oceanogr. 55, 965–972.

Chen, B.Z., et al., 2009. Estuarine nutrient loading affects phytoplankton growth and microzooplankton grazing at two contrasting sites in Hong Kong coastal waters. Mar. Ecol. Prog. Ser. 379, 77–90.

Chen, Y.L.L., Chen, H.Y., 2006. Seasonal dynamics of primary and new production in the northern South China Sea: the significance of river discharge and nutrient advection. Deep-Sea Res. 53, 971–986.

Chisholm, S.W., 1992. Phytoplankton size. In: Falkowski, P.G., Woodhead, A.D. (Eds.), Primary Productivity and Biogeochemical Cycles in the Sea. Plenum Press, New York, pp. 213–237.

Christaki, U., Jacquet, S., Dolan, J.R., Vaulot, D., Rassoulzadegan, F., 1999. Growth and grazing on *Prochlorococcus* and *Synechococcus* by two marine ciliates. Limnol. Oceanogr. 44, 52–61.

Durand, M.D., Olson, R.J., Chisholm, S.W., 2001. Phytoplankton population dynamics at the Bermuda Atlantic Time-series station in the Sargasso Sea. Deep-Sea Res. II 48, 1983–2003.

Fang, G., Fang, W., Fang, Y., Wang, K., 1998. A survey of studies on the South China Sea upper ocean circulation. Acta Oceanogr. Taiwanica 37, 1–16.

Finkel, Z.V., Sebbo, J., Feist-Burkhardt, S., Irwin, A.J., Katz, M.E., Schofield, O.M.E., Falkowksi, P.G., 2007. A universal driver of macroevolutionary change in the size of marine phytoplankton over the Cenozoic. Proc. Natl. Acad. Sci. USA 104, 20416–20420.

Finkel, Z.V., Vaillancourt, C.J., Irwin, A.J., Reavie, E.D., Smol, J.P., 2009. Environmental control of diatom community size structure varies across aquatic ecosystems. Proc. R. Soc. B 276, 1627–1634.

Follows, M.J., Dutkiewicz, S., Grant, S., Chisholm, S.W., 2007. Emergent biogeography of microbial communities in a model ocean. Science 315, 1843–1846.

Furuya, K., Hayashi, M., Yabushita, Y., 1998. HPLC determination of phytoplankton pigments using N,N-dimethylfolmamide. J. Oceanogr. 54, 199–203.

Gan, J.P., Lu, Z., Dai, M., Cheung, A.Y.Y., Liu, H., Harrison, P.J., 2010. Biological response to intensified upwelling and to a river plume in the northeastern South China Sea: A modeling study. J. Geophys. Res. 115, C09001. doi:10.1029/2009JC005569.

Garrison, D.L., Gowing, M.M., Hughes, M.P., Campbell, L., Caron, D.A., Dennett, M.R., Shalapyonok, A., Olson, R.J., Landry, M.R., Brown, S.L., Liu, H.-B., Azam, F., Steward, G.F., Ducklow, H.W., Smith, D.C., 2000. Microbial food web structure in the Arabian Sea: a US JGOFS study. Deep-Sea Res. II 47, 1387–1422.

Hu, J., Kawamura, H., Hong, H., Qi, Y., 2000. A review on the Currents in the South China Sea: seasonal circulation, South China Sea warm current and Kuroshio Intrusion. J. Oceanogr. 56, 607–624.

Irwin, A.J., Finkel, Z.V., 2008. Mining a sea of data: deducing the environmental controls of ocean chlorophyll. Plos One 3, e3836. doi:10.1371/journal.pone.0003836.

Jing, H., Liu, H., Suzuki, K., 2009. Phylogenetic diversity of marine *Synechococcus* spp. in the sea of Okhotsk. Aquat. Microb. Ecol. 56, 55–63.

Jing, H., Liu, H., Bird, D.F., Wong, T.H.C., Chen, X., Chen, B., 2010. Composition and seasonal variability of picoeukaryote communities at two subtropical coastal sites with contrasting trophic conditions. J. Plankton Res. 32, 565–573.

Johnson, Z.I., Zinser, E.R., Coe, A., McNulty, N.P., Woodward, E.M.S., Chisolmn, S.W., 2006. Niche partitioning among *Prochlorococcus* ecotypes along ocean-scale environmental gradients. Science 311, 1737–1740.

Li, W.K.W., 1998. Annual average abundance of heterotrophic bacteria and *Synechococcus* in surface ocean waters. Limnol. Oceanogr. 43, 1746–1753.

Li, W.K.W., 2002. Macroecological patterns of phytoplankton in the northwestern North Atlantic Ocean. Nature 419, 154–157.

Li, W.K.W., Dickie, P.M., 2001. Monitoring phytoplankton, bacterioplankton, and virioplankton in a coastal inlet (Bedford Basin) by flow cytometry. Cytometry 44, 236–246.

Liu, A.K., Chang, Y.S., Hsu, M.K., Liang, N.K., 1998. Evolution of nonlinear internal waves in the East and South China Seas. J. Geophys. Res. 103 (C4), 7995–8008.

Liu, H., Bidigare, R.R., Laws, E.A., Landry, M.R., Campbell, L., 1999. Cell cycle and physiological characteristics of *Synechococcus* (WH7803) in chemostat culture. Mar. Ecol. Prog. Ser. 189, 17–25.

Liu, H., Campbell, L., Landry, M.R., Nolla, H.A., Brown, S.L., Constantinou, J., 1998. *Prochlorococcus* and *Synechococcus* growth rates and contribution to production in the Arabian Sea during the 1995 Southwest and Northeast monsoons. Deep-Sea Res. II 45, 2327–2352.

Liu, H., Chang, J., Tseng, C.M., Wen, L.S., Liu, K.K., 2007. Seasonal variability of picoplankton in the northern South China Sea at the SEATS station. Deep-Sea Res. II 54, 1602–1616.

Liu, H., Imai, K., Suzuki, K., Nojiri, Y., Tsurushima, N., Saino, T., 2002a. Seasonal variability of picophytoplankton and bacteria in the western subarctic Pacific Ocean at station KNOT. Deep-Sea Res. II 49, 5409–5420.

Liu, K.K., Chao, S.Y., Shaw, P.T., Gong, G.C., Chen, C.C., Tang, T.Y., 2002b. Monsoon-forced chlorophyll distribution and primary production in the South China Sea: observations and a numerical study. Deep-Sea Res. I 49, 1387–1412.

Mann, E.L., Ahlgren, N., Moffett, J.W., Chisholm, S.W., 2002. Copper toxicity and cyanobacteria ecology in the Sargasso Sea. Limnol. Oceanogr. 47, 976–988.

Moore, L.R., Goericke, R., Chisholm, S.W., 1995. Comparative Physiology of *Synechococcus* and *Prochlorococcus*—influence of light and temperature on growth, pigments, fluorescence and absorptive properties. Mar. Ecol. Prog. Ser. 116, 259–275.

Moore, L.R., Post, A.F., Rocap, G., Chisholm, S.W., 2002. Utilization of different nitrogen sources by the marine cyanobacteria *Prochlorococcus* and *Synechococcus*. Limnol. Oceanogr. 47, 989–996.

Moore, L.R., Rocap, G., Chisholm, S.W., 1998. Physiology and molecular phylogeny of coexisting *Prochlorococcus* ecotypes. Nature 393, 464–467.

Montagnes, D.J.S., Franklin, D.J., 2001. Effect of temperature on diatom volume, growth rate, and carbon and nitrogen content: reconsidering some paradigms. Limnol. Oceanogr. 46, 2008–2018.

Morel, A., Ahn, Y.-H., Partensky, F., Vaulot, D., Claustre, H., 1993. *Prochlorococcus* and *Synechococcus*: a comparative study of their optical properties in relation to their size and pigmentation. J. Mar. Res. 51, 617–649.

Morel, A., 1991. Optics of marine particles and marine optics. In: Demers, S. (Ed.), Proceedings of the NATO Advanced Study Institute of Individual Cell and

Particle Analysis in Oceanography. Aquafreda di Maratea Italy, 21–30 October 1990. Springer, Berlin, pp. 141–188.
Ning, X., Chai, F., Xue, H., Cai, Y., Liu, C., Shi, J., 2004. Physical-biological oceanographic coupling influencing phytoplankton and primary production in the South China Sea. J. Geophys. Res. 109, C10005. doi:10.1029/2004JC002365.
Ning, X., Li, W.K.W., Cai, Y.M., Shi, J., 2005. Comparative analysis of bacterioplankton and phytoplankton in three ecological provinces of the northern South China Sea. Mar. Ecol. Prog. Ser. 293, 17–28.
Olson, R.J., Chisholm, S.W., Zettler, E.R., Altabet, M.A., Dusenberry, J.A., 1990. Spatial and temporal distributions of prochlorophyte picoplankton in the North Atlantic Ocean. Deep-Sea Res. 37, 1033–1051.
Olson, R.J., Zettler, E.R., DuRand, M.D., 1993. Phytoplankton analysis using flow cytometry. In: Kemp, P., Sherr, B.F., Sherr, E.B., Cole, J.J. (Eds.), Handbook of Methods in Aquatic Microbial Ecology. Lewis Publishers, New York, pp. 175–186.
Paerl, H.W., Huisman, J., 2008. Climate–blooms like it hot. Science 320, 57–58.
Pan, L.A., Zhang, J., Chen, Q., Deng, B., 2006. Picoplankton community structure at a coastal front region in the northern part of the South China Sea. J. Plankton Res. 28, 337–343.
Parsons, T.R., Maita, Y., Lalli, C.M., 1984. A Manual of Chemical and Biological Methods for Seawater Analysis. Pergamon, New York.
Raven, J.A., 1998. The twelfth Tansley Lecture. Small is beautiful: the picophytoplankton. Funct. Ecol. 12, 503–513.
Rocap, G., Larimer, F.W., Lamerdin, J., Malfatti, S., Chain, P., Ahlgren, N.A., Arellano, A., Coleman, M., Hauser, L., Hess, W.R., Johnson, Z.I., Land, M., Lindell, D., Post, A.F., Regala, W., Shah, M., Shaw, S.L., Steglich, C., Sullivan, M.B., Ting, C.S., Tolonen, A., Webb, E.A., Zinser, E.R., Chisholm, S.W., 2003. Genome divergence in two *Prochlorococcus* ecotypes reflects oceanic niche differentiation. Nature 424, 1042–1047.
Sullivan, M.B., Waterbury, J.B., Chisholm, S.W., 2003. Cyanophages infecting the oceanic cyanobacterium *Prochlorococcus*. Nature 426, 584.
Wang, L., et al., 1999. East Asian monsoon climate during the Late Pleistocene: high-resolution sediment records from the south China Sea. Mar. Geol. 156, 245–284.
Waterbury, J.B., Watson, S.W., Valois, F.W., Franks, D.G., 1986. Biological and ecological characterization of the marine unicellular cyanobacterium *Synechococcus*. In: Platt, T., Li, W. (Eds.), Photosynthetic Phyloplanklon. Canadian Bulletin of Fisheries and Aquatic Science, Ottawa, pp. 71–120.
Wong, G.T.F., Ku, T.L., Mulholland, M., Tseng, C.M., Wang, D.P., 2007. The SouthEast Asian Time-series Study (SEATS) and the biogeochemistry of the South China Sea—an overview. Deep-Sea Res. II 54, 1434–1447.
Worden, A.Z., Binder, B.J., 2003. Application of dilution experiments for measuring growth and mortality rates among *Prochlorococcus* and *Synechococcus* populations in oligotrophic environments. Aquat. Microb. Ecol. 30, 159–174.
Worden, A.Z., Nolan, J.K., Palenik, B., 2004. Assessing the dynamics and ecology of marine picophytoplankton: the importance of the eukaryotic component. Limnol. Oceanogr. 49, 168–179.
Wu, J.F., et al., 2003. Dissolved inorganic phosphorus, dissolved iron, and *Trichodesmium* in the oligotrophic South China Sea. Global Biogeochem. Cycles 17, 1008. doi:10.1029/2002GB001924.
Zubkov, M.V., Fuchs, B.M., Tarran, G.A., Burkill, P.H., Amann, R., 2003. High rate of uptake of organic nitrogen compounds by *Prochlorococcus* cyanobacteria as a key to their dominance in oligotrophic oceanic waters. Appl. Environ. Microbiol. 69, 1299–1304.
Zubkov, M.V., Sleigh, M.A., Burkill, P.H., Leakey, R.J.G., 2000. Picoplankton community structure on the Atlantic Meridional Transect: a comparison between seasons. Prog. Oceanogr. 45, 369–386.
Zubkov, M.V., Sleigh, M.A., Tarran, G.A., Burkill, P.H., Leakey, R.J.G., 1998. Picoplanktonic community structure on an Atlantic transect from 50 degrees N to 50 degrees S. Deep-Sea Res. I 45, 1339–1355.